# Polymer Chemistry

Accepted Manuscript






ROYAL SOCIETY OF CHEMISTRY

www.rsc.org/polymers

# Novel Metallo-Dendrimers Containing Various Ru Core Ligands and Dendritic Thiophene Arms for Photovoltaic Applications

**Rudrakanta Satapathy,[a] Mohan Ramesh,[a] Harihara Padhy,[a] I-Hung Chiang,[a] Chih-Wei Chu,*[bc] Kung-Hwa Wei[a] and Hong-Cheu Lin*[a]**

Three series of supramolecular mono- (i.e., **Ru1G1, Ru1G2** and **Ru1G3**), bis- (i.e., **BTRu2G1, BTRu2G2** and **BTRu2G3**) and tris- (i.e., **TPARu3G1, TPARu3G2** and **TPARu3G3**) 'Ru'-based dendritic complexes were synthesized. Their photophysical and electrochemical properties were investigated. These metallo-dendritic complexes covered a broad absorption range of 250-750 nm with the optical bandgaps of 1.51-1.86 eV. The energy levels of the metallo-dendrimers can be effectively adjusted not only by different generations of dendritic thiophene arms but also their π-conjugated core ligands bearing various electron donor (i.e., triphenylamine) and acceptor (i.e., benzothiadiazole) moieties. Due to the donor-acceptor effect, the bis-'Ru'-based dendrimers containing a benzothiadiazole electron-acceptor core ligand showed the highest power conversion efficiency (PCE) among these three series of metallo-dendrimers. Tris-'Ru'-based architecture with a triphenylamine electron-donor core ligand revealed moderate photovoltaic performance. Among different generations (**G1-G3**) of dendrimers, the third generation (**G3**) possessed the highest PCE values in each series of 'Ru'-based dendrimers. Hence, the third generation of bis-'Ru'-based dendrimer **BTRu2G3** blended with $PC_{70}BM$ (1:3 w/w) showed the highest PCE value of 0.77% (without any aids of additives or annealing), which is the highest efficiency among all bulk hetero-junction (BHJ) solar cells containing metallo-dendrimers reported so far.

## Introduction

The design of supramolecular assemblies possessing novel functional properties of tailored non-covalent structures are of growing interests in current researches.[1] Especially, oligo-pyridyl ligands and their transition metal complexes have been developed ample applications, such as active materials in self-assembled molecular devices, electroluminescent materials in molecular electronics and photonics, luminescent sensor materials in molecular biology and medical diagnostics.[1] Directional and effective electron energy transfers could be achieved by the design of suitable multiple ligands and its complexation with transition metal ions. Among N-heterocyclic ligands, the remarkably high affinities of 2,2':6',2"-terpyridine towards transition-metal ions and chelation effects due to dπ-pπ* back-bonding of the metal ions to pyridyl rings make them useful for supramolecular constructions. Compared with other transition metal ion complexes, due to the high binding strength of Ru(II) with the terpyridyl moiety, the Ru(II) complexes show a remarkable stability and can only be cleaved under extreme conditions like low pH values, high temperatures and additions of strong competitive ligands.[2] Suitable π-conjugated substituents at the 4'-position of the 2,2':6',2"-terpyridyl unit exhibit intriguing spectroscopic and redox properties which cause effective electronic communications between the metal ions and π ligands.[3] Moreover, their photophysical, electrochemical and magnetic properties are strongly influenced by the natures of the π-conjugated moieties attached to the terpyridyl units.[3] Furthermore, the electronic communications between the metal-complexed terpyridines with the attached π-conjugated moieties are additional fascinating features directing their potentials for the designs of new supramolecular architectures. Recently, terpyridyl Ru(II) complexes have gained interests for the researchers to investigate their photovoltaic cell (PVC) applications.[4] Likewise, dyadic Ru(II) complexes consisting of 4'-substituted terpyridyl units have been utilized as specifically active candidates in organic photovoltaic cells.[5] These systems received extensive attentions owing to their very long-lived metal to ligand charge transfer (MLCT) excited states and high molar extinction coefficients in the visible range.[5] In these dyads, the excited state that is generated upon the absorption of light leads to a charge separated state with a high efficiency.[6] During the synthesis of dyadic polymers, the large polydispersities and poor solubilities might be arisen due to the various polymeric sizes (as well as molecular weights) and highly conjugated metallo-polymers, respectively, which could extensively amend the carrier mobilities of the OPV devices.[6a,b] Therefore, monodispersed materials are desirable to obtain efficient charge transports and device efficiencies in organic photovoltaic applications because of their aptitudes to control the morphologies of blends.[6c] In this esteem, conjugated dendrimers offer an alternative to the conjugated polymers to be useful in organic photovoltaics6d because of the following advantages. Dendrimers[6] (1) possess well-defined molecular weights with monodispersity; (2) have shape persistency, which allows to maintain their structures in a solution-processable form; (3) can be synthesized with high purities compared with their polymeric derivatives; (4) own internal local electric fields which may be created during the charge transfer from the peripheral arms to the cores of dendrimers. In addition, conjugated dendrimers are

[a] Department of Materials Science and Engineering, National Chiao Tung University, Hsinchu, Taiwan (ROC). E-mail: linhc@cc.nctu.edu.tw.
[b] Research Center for Applied Sciences, Academia Sinica, Taipei, Taiwan (ROC). E-mail: gchu@gate.sinica.edu.tw.
[c] Department of Photonics, National Chiao Tung University, Hsinchu, Taiwan (ROC).

expected to show a high degree of ordering in OPV devices due to their small size and monodisperse nature. To the best of our knowledge, however, there are only a few reports on the applications of dendrimers for organic solar cells.[7a-c] Metal-based supramolecular architectures for the development of bulk hetero-junction BHJ) solar cells are under progress.[7d] Due to the three dimensional hyper-branched structure, the branches become denser with increasing distance from the core, which produces shell effects on dendrimers.[8] Thus, high-generation dendrimers possessing highly dense branches towards the outer surfaces may act as a barrier to restrict the charge transfers between the inner and outer parts of the dendrimers. Thiophene dendrimers and terpyridyl dendritic complexes have recently attained promising attentions for the applications of photovoltaic and other optoelectronic applications.[8]

On the aim towards developing the metallo-dendrimers for BHJ solar cell applications, mono- (i.e., **Ru1G1**, **Ru1G2** and **Ru1G3**), bis- (i.e., **BTRu2G1**, **BTRu2G2** and **BTRu2G3**) and tris- (i.e., **TPARu3G1**, **TPARu3G2** and **TPARu3G3**) 'Ru'-ba**sed** dendritic complexes were prepared and characterized. We have compared their photo physical and photo voltaic properties in relation to their structural architecture.

Experimental Section

**Synthetic procedures**

***G1-SnBu$_3$.*** **G1** (2.1 gm, 5.03 mmole) was dissolved in 25 mL THF and cooled to -78°C. To it 2.5 M n-BuLi in hexane (2.41 mL, 6.04 mmole) was added drop wise. The reaction was allowed stir at -78°C for 1 hour. To it $SnBu_3Cl$ (1.96 gm, 1.63 mL, 6.03mmole) was added rapidly. The reaction mixture was allowed to warm to room temperature and stirred overnight. The reaction mixture was quenched by addition of 20 mL $H_2O$ and extracted by ethyl acetate via three times water wash. The organic layer was dried over $MgSO_4$, solvent was removed by rotary evaporation to get the crude product as pale-yellow oil. The crude product was used for next step without further purification. $^1$H NMR ($CDCl_3$, 300 MHz): 7.10 (s, 1H), 6.91 (d, 1H, 3.3 Hz), 6.87 (d, 1H, 3.6 Hz), 6.66 (d, 2H, 3.3 Hz), 2.77 (m, 4H), 1.64 (m, 4H), 1.56 (m, 6H), 1.36 (t, 6H, 7.3Hz), 1.30 (m, 12H), 1.11 (t, 6H, 8.3 Hz), 0.90 (m, 15H).

***G1-TPY.*** **G1-SnBu3** (3.5 gm, 4.95 mmole), 4'-(5-bromo-4-dodecylthiophen-2-yl)-2,2':6',2"-terpyridine (1.62 gm,4.13 mmole) and $Pd(PPh_3)_4$ (114 mg, 0.099 mmole) was taken in a two neck flask and degassed by nitrogen. 30 mL dry DMF was poured into it and the reaction mixture heated to 90°C overnight. 100 mL of water was added to it and the reaction mixture was extracted by EA. Organic layer was dried over $MgSO_4$ and the solvent was removed by rotary evaporation. Crude product was purified by neutral alumina column chromatography using hexane: EA = 15:1 to yield pure compound (2.02 gm, 67.1%). $^1$H NMR ($CDCl_3$, 300 MHz) : 8.75 (d, 2H, 6 Hz), 8.67 (s, 2H), 8.65 (d, 2H, 6 Hz), 7.90 (dt, 2H, 9 Hz ,1.2 Hz), 7.71 (1H, 3.9 Hz), 7.38 (2H, 6 Hz), 7.27 (s, 1H), 7.23 (d, 1H, 3 Hz), 6.98 (d, 1H, 3 Hz), 6.92 (d, 1H, 3 Hz), 6.69 (d, 2H, 3 Hz), 2.82 (t, 4H, 7.5 Hz ), 1.70-1.61 (m, 4H), 1.39-1.26 (m, 12H), 0.94 (t, 6H, 6.5 Hz). $^{13}$C NMR ($CDCl_3$, 300MHz) : 155.98, 155.88, 149.07, 147.73, 146.41, 142.80, 140.45, 138.32, 136.78, 134.58, 134.28, 132.44, 131.94, 131.11, 127.52, 126.67, 126.57, 126.41, 124.68, 124.23, 124.08, 123.85, 121.24, 116.56, 31.55, 31.52, 31.47, 28.74, 26.81, 22.57, 17.48, 14.07, 13.58 Elemental analysis for $C_{43}H_{43}N_3S_4$: Calculated: (%) C, 70.74; H, 5.94; N, 5.76. Found: (%) C, 70.29; H, 5.93; N, 5.90. MS (FAB): m/z 730 (calcd $(M)^+$).

***G2-SnBu$_3$.*** **G1** (1.8 gm, 1.97 mmole) was dissolved in 25 mL THF and cooled to -78°C. To it 2.5 M n-BuLi in hexane (0.94 mL, 2.36 mmole) was added drop wise. The reaction was allowed stir at -78°C for 1 hour. To it $SnBu_3Cl$ (0.83 gm, 0.69 mL, 2.56 mmole) was added rapidly. The reaction mixture was allowed to warm to room temperature and stirred overnight. The reaction mixture was quenched by addition of 20 mL $H_2O$ and extracted by ethyl acetate via three times water wash. The organic layer was dried over $MgSO_4$, solvent was removed by rotary evaporation to get the crude product as pale-yellow oil. The crude product was used for next step without further purification. $^1$H NMR ($CDCl_3$, 300 MHz): 7.19 (s, 1H), 7.18 (s, 1H), 7.15 (s, 1H), 6.93 (t, 2H, 3 Hz), 6.87 (d, 2H, 3 Hz), 6.65 (m, 4H), 2.76 (t, 8H, 6.9 Hz), 1.69-1.57 (m, 14H), 1.36-1.29 (m, 30H), 1.11 (t, 6H, J=8.2 Hz), 0.89 (m, 21H).

***G$_2$-TPY***: **G$_2$-SnBu$_3$** (2.3 gm, 1.91 mmole), 4'-(5-bromo-4-dodecylthiophen-2-yl)-2,2':6',2"-terpyridine (0.62 gm, 1.59 mmole) and $Pd(PPh_3)_4$ (44 mg, 0.038 mmole) was taken in a two neck flask and degassed by nitrogen .25 mL dry DMF was poured into it and the reaction mixture heated to 90°C overnight. 100 mL of water was added to it and the reaction mixture was extracted by EA. Organic layer was dried over $MgSO_4$ and the solvent was removed by rotary evaporation. Crude product was purified by neutral alumina column chromatography using (hexane: EA = 20:1) to yield pure compound (1.27 gm, 54.2%). $^1$H NMR ($CDCl_3$, 300 MHz): 8.75 (d, 2H, 6 Hz), 8.67 (s, 2H), 8.65 (d, 2H ,6 Hz), 7.90 (dt, 2H, 9 Hz, 1.2 Hz), 7.71 (1H, 3.9 Hz), 7.38 (2H, 6 Hz), 7.27 (s, 1H), 7.23 (d, 1H, 3 Hz), 6.98 (d, 1H, 3 Hz), 6.92 (d, 1H, 3 Hz) 6.69 (d, 2H, 3 Hz), 2.82 (t, 4H, 7.5 Hz), 1.70-1.61 (m, 4H), 1.39-1.26 (m, 12H), 0.94 (t, 6H, 6.5 Hz). $^{13}$C NMR ($CDCl_3$, 300 MHz): 155.76, 155.72, 148.97, 147.62, 147.41 146.27, 146.09,142.43, 140.79, 137.65, 136.67, 135.61, 134.75, 134.48, 134.39, 132.19, 131.91, 131.87, 131.81, 130.24, 129.70, 127.59, 127.49, 126.51, 126.44, 126.26, 124.19, 124.05, 123.77, 121.16, 116.39, 116.20, 31.61, 31.51, 30.16, 28.82, 28.80, 27.83, 26.86, 25.60, 22.71, 22.63, 14.35, 13.64. Elemental analysis for $C_{71}H_{75}N_3S_8$: Calculated: (%) C, 69.51; H, 6.16; N, 3.42. Found: (%) C, 69.32; H, 6.63; N, 3.41. MS (FAB): m/z 1227 (calcd $(m)^+$).

***G$_3$-SnBu$_3$.*** **G$_3$** (1.5 gm, 0.78 mmole) was dissolved in 20 mL THF and cooled to -78°C. To it 2.5 M n-BuLi in hexane (0.37 mL, 0.93 mmole) was added drop wise. The reaction was allowed stir at -78°C for 1 hour. To it $SnBu_3Cl$ (0.33 gm, 0.27 mL, 1.04 mmole) was added rapidly. The reaction mixture was allowed to warm to room temperature and stirred overnight. The reaction mixture was quenched by addition of 20 mL $H_2O$ and extracted by ethyl acetate via three times water wash. The organic layer was dried over $MgSO_4$, solvent was removed by rotary evaporation to get the crude product as pale-yellow oil. The crude product was used for next step without further purification.

***G$_3$-TPY.*** **G$_2$-SnBu$_3$** (1.7 gm, 0.77 mmole), 4'-(5-bromo-4-dodecylthiophen-2-yl)-2,2':6',2"-terpyridine (0.25 gm, 0.64 mmole) and $Pd(PPh_3)_4$ (17.8 mg, 0.015 mmole) was taken in a two neck flask and degassed by nitrogen. Dry DMF (15 mL) was poured into it and the reaction mixture heated to 90°C overnight. 100 mL of water was added to it and the reaction mixture was extracted by EA. Organic layer was dried over $MgSO_4$ and the solvent was removed by rotary evaporation. Crude product was purified by neutral alumina column chromatography using (hexane: EA = 20:1) to yield pure compound (0.82 g, 48.2%). $^1$H NMR ($CDCl_3$, 300 MHz): 8.72 (d, 2H, 6 Hz), 8.65 (s, 2H), 8.62 (d, 2H, 9 Hz), 7.77 (t, 2H, 9 Hz), 7.59 (d, 3 Hz), 7.29-7.24 (m, 7H), 7.18 (s, 1H),7.12 (d, 1H, 2.7 Hz), 7.02 (s, 1H), 6.97 (m, 4H), 6.91 (m, 4H), 6.65 (m, 8H), 2.74 (t, 16H, 7.4 Hz), 1.63 (m, 16H), 1.34 (m, 48H), 0.96 (t, 24H, 5.4 Hz). $^{13}$C NMR ($CDCl_3$, 300 MHz): 155.98, 155.82, 149.06, 147.60, 147.35, 147.29, 146.23, 146.19, 146.06, 146.02, 142.66, 141.13, 137.65, 136.79, 136.11, 135.30, 134.76, 134.46, 134.42, 134.36, 133.17, 133.08, 132.95, 132.58, 132.31, 132.21, 132.16, 131.95, 131.86, 131.72, 131.37, 131.31, 130.47, 130.39, 130.26, 129.73, 129.59, 127.64, 127.52, 126.66, 126.43, 126.39, 126.25, 125.26, 124.10, 123.94, 121.25, 116.65, 31.54,31.46, 30.14, 30.10, 28.77, 22.57, 14.05. Elemental analysis for $C_{127}H_{139}N_3S_{16}$: Calculated : (%) C, 68.69; H, 6.31; N, 1.89. Found: (%) C, 67.86; H, 6.75; N, 1.73. MS (MALDI-TOF): m/z 2220.7 (calcd $(M)^+$) .

***G1-TPY-RuCl$_3$.*** **G1-TPY** (600 mg, 0.822 mmole) and $RuCl_3 .xH_2O$ (236.46 mg, 0.906 mmole) were taken in MeOH: THF/ 5:1 under $N_2$ atmosphere. The mixture was refluxed overnight. The solid residue was filtered, washed in excess methanol and dried to get the product as shiny black solid (746.04 mg, 97%).

***G2-TPY-RuCl$_3$.*** **G1-TPY** (500 mg, 0.407 mmole) and $RuCl_3 .xH_2O$ (117 mg, 0.448 mmole) were taken in MeOH: THF /5:1 (100 ml) under $N_2$ atmosphere. The mixture was refluxed overnight. The solid residue was filtered, washed in excess methanol and dried to get the product as black solid (574.28 mg, 98.5%).

***G2-TPY-RuCl$_3$.*** **G2-TPY** (400 mg, 0.18 mmole) and $RuCl_3 .xH_2O$ (51.15 mg, 0.196 mmole) were taken in MeOH: THF /5:1 (100 mL) under $N_2$ atmosphere. The mixture was refluxed overnight. The solid residue was filtered, washed in excess methanol and dried to get the product as black solid (420.52 mg, 96.4%).

***Ru1G1.*** **G1-TPY-RuCl$_3$** (360 mg, 0.385 mmole) and $AgBF_4$ (300 mg, 1.54 mmole) were taken in acetone (60 mL) and refluxed 18 hrs under $N_2$ atmosphere. The solution was filtered to remove AgCl salt. The filtrate was evaporated and to it G1-TPY (280 mg, 0.385 mmole) was added. The mixture was dissolved in 5 mL dimethyl acetamide and 50 mL n-BuOH and refluxed for 24 hours. The product was cooled and added drop wise into a beaker containing 500 mL MeOH under stirring. The solid was filtered, washed in MeOH and 5:1 mixture of MeOH: acetone. The residue was dried to get dark red solid (560.04 mg, 93.2%). $^1$H NMR (DMSO-$d_6$, 300 MHz): 9.33 (s, 4H), 9.11 (d, 4H, 8.1 Hz), 8.48 (d, 2H, 3.9 Hz), 8.07 (t, 4H, 7.5 Hz), 7.82 (d, 2H, 3.6 Hz), 7.72 (s, 2H), 7.60 (d, 4H, 6 Hz), 7.28 (t, 4H, 6.2 Hz), 7.12 (d, 4H, 3.6 Hz), 6.87 (d, 2H, 3.6 Hz), 6.85 (d, 2H, 3.3 Hz), 2.78 (t, 8H, 7.5 Hz), 1.60-1.57 (m, 8H), 1.35-1.24 (m, 24H), 0.86 (t, 12H, 6.6 Hz). Elemental analysis for $C_{86}H_{86}N_6RuS_8$: Calculated: C, 66.16; H, 5.55; N, 5.38. Found: (%) C, 66.86; H,5.75; N, 5.43. MS (MALDI-TOF): m/z 1559.24, (calcd $(M)^+$: 1560.37).

***Ru1G2.*** **G2-TPY-RuCl$_3$** (340 mg, 0.237 mmole) and $AgBF_4$ (194.67 mg, 0.949 mmole) were taken in acetone (50 mL) and refluxed 20 hours under $N_2$ atmosphere. The solution was filtered to remove AgCl salt. The filtrate was evaporated and to it **G2-TPY** (290.3 mg, 0.237 mmole) was added. The mixture was dissolved in 5 mL dimethyl acetamide and 50 mL n-BuOH and refluxed for 24 hours. The product was cooled and added drop wise into a beaker containing 500 mL MeOH under stirring. The solid was filtered, washed in MeOH and 6:1 mixture of MeOH: acetone. The residue was dried to get dark red solid (559.77 mg, 94.1%). $^1$H NMR (DMSO-d6, 300 MHz): 9.35-9.28 (br, 4H), 9.11 (d, 4H, 8.1 Hz), 8.50-8.43 (br, 2H), 8.07 (br, 4H), 7.90-7.83 (br, 4H), 7.58-7.49 (br, 10H), 7.38-7.28 (br, 4H), 7.05-7.02 (br, 8H), 6.82-6.78 (br, 8H), 2.77-2.74 (br, 16H), 1.57-1.55 (br, 16H), 1.27 (br, 48H), 0.85 (br, 24H). Elemental analysis for $C_{142}H_{150}N_6RuS_{16}$: Calculated: C, 66.76; H, 5.92; N, 3.29. Found: (%) C, 66.16; H,5.25; N, 3.73. MS (MALDI-TOF): m/z 2554.58, (calcd $(M)^+$: 2553.65).

***Ru1G3.*** **G3-TPY-RuCl$_3$** (7.2 mg, 0.18 mmole) and $AgBF_4$ (140 mg, 0.721 mmole) were taken in acetone (50 mL) and refluxed 20 hours under $N_2$ atmosphere. The solution was filtered to remove AgCl salt. The filtrate was evaporated and to it **G3-TPY** (400 mg, 0.18 mmole) was added. The mixture was dissolved in 5 mL dimethyl acetamide and 50 mL n-BuOH and refluxed for 24 hours. The product was cooled and added drop wise into a beaker containing 500 mL MeOH under stirring. The solid was filtered, washed in MeOH and 6:1 mixture of MeOH: acetone. The residue was dried to get dark red solid (749.72 mg, 91.7%). $^1$H NMR ($CDCl_3$, 300 MHz): 8.85 (br, 4H), 8.70-8.62 (br, 4H), 8.16 (br, 2H), 7.86 (br, 4H), 7.41 (br, 4H), 7.24-7.05 (br, 20H), 6.90-6.82 (br, 16H), 6.61-6.57 (br, 16H), 2.73-2.69 (br, 32H), 1.65-1.58 (br, 32H), 1.26 (br, 96H), 0.85 (br, 48H). Elemental Analysis for $C_{254}H_{278}N_6RuS_{32}$: Calculated: C, 67.17; H, 6.17; N, 1.85Found: (%) C, 66.16; H,5.25; N, 3.73. MS (MALDI-TOF): m/z 4537.05, (calcd $(M)^+$: 4541.21).

*Synthesis of Core Ligand for Double Metal System*

The core ligand for the double metal system was prepared by our previously reported procedure.[5c]

*General Synthetic Procedure of Double Metal Systems.*

**G-TPY-RuCl$_3$** (2.1 equiv. w.r.t. **BT2TPY**) and $AgBF_4$ (6.4 equiv. w.r.t. **TPA3TPY**) were taken in acetone (50 mL) and refluxed 36 hrs under $N_2$ atmosphere. The solution was filtered to remove AgCl salt. The filtrate was evaporated and to it **BT2TPY** (1 equiv.) was added. The mixture was dissolved in 5 mL dimethyl acetamide and 50 mL n-BuOH and refluxed for 48 hours. The product was cooled and added drop wise into a beaker containing 500 mL MeOH under stirring. The solid was filtered, washed in MeOH and 6:1 mixture of MeOH:acetone. The residue was dried and recrystallized in mixture of acetone:MeOH (1:10) to get desired compounds.

***BTRu2G1.*** Black powder. Yield: 59.6 %. $^1$H NMR (DMSO-$d_6$, 300 MHz): 9.37-9.35 (br, 8H), 9.10 (br, 8H), 8.56-8.47 (m, br, 8H), 8.39-8.32 (m, br, 8H), 8.23-8.07 (m, br, 8H), 7.93-7.68 (m, br, 6H), 7.59-7.47 (m, br, 6H), 7.28 (s, br, 2H), 7.19-7.10 (m, br, 4H), 6.86-6.64 (m, br,4H), 2.76-2.62 (m, br, 12H), 1.54-1.42 (m, br, 12H), 1.32-1.20 (m, br, 36H), 0.90-0.81 (m, br, 18H). MS (MALDI-TOF): m/z 2756.15 (calcd $(M)^+$: 2757.59).

***BTRu2G2.*** Black Powder. Yield: 55.2%. $^1$H NMR (DMSO-$d_6$, 300 MHz): 9.35 (br, 8H), 9.10 (br, 8H), 8.52-8.49 (m, br, 8H), 8.32-8.23 (m, br, 8H), 8.07 (m, br, 8H), 7.92-7.89 (m, br, 6H), 7.75-7.48 (m, br, 7H), 7.40-7.28 (m, br, 5H), 7.04-7.02 (m, br, 8H), 6.87-6.78 (m, br, 8H), 2.76-2.71 (m, br, 20H), 1.58-1.42 (m, br, 20H), 1.25-1.19 (m, br, 60H), 0.85-0.76 (m, br, 30H). MS (MALDI-TOF): m/z 3752.55 (calcd $(M)^+$: 3751.87).

***BTRu2G3.*** Black Powder. Yield: 51.3%. $^1$H NMR (DMSO-$d_6$, 300 MHz): 9.35-9.24 (br, 8H), 9.11 (br, 8H), 8.76-8.63 (m, br, 8H), 8.49-8.22 (m, br, 8H), 8.06-8.00 (m, br, 8H), 7.86-7.51 (m, br, 14H), 7.53-7.29 (m, br, 12H), 7.01-6.87 (m, br, 16H), 6.66 (m, br, 16H), 2.77-2.73 (m, br, 36H), 1.57-1.41 (m, br, 36H), 1.27-1.25 (m, br, 108H), 0.84-0.72 (m, br, 54H). MS (MALDI-TOF): m/z 5735.05 (calcd $(M)^+$: 5738.42).

*Synthesis of Core Ligand for Triple Metal System*

*2-Bromo-3-dodecylthiophene*. 3-hexylthiophene (5.2 gm, 20.59 mmole) was dissolved in 250 mL of THF and was cooled in an ice bath. NBS (3.66 gm, 20.59 mmol) was added in one portion. Stirring was continued in the ice bath for 1 h and the mixture was poured into water. Organic layer was extracted with hexanes two times (50 mL x 2) and the dried over $MgSO_4$. Solvent was removed under reduced pressure and the crude oil, was purified by column chromatography on silica gel to afford 6.47g of compound (94.9%). $^1$H NMR ($CDCl_3$, 300 MHz): 7.19 (d, 1H, 5.6 Hz), 6.80 (d, 1H, 5.6 Hz), 2.55 (t, 2H, 7.5 Hz), 1.59-1.54 (m, 2H), 1.29-1.25 (m, 18H), 0.88 (t, 3H, 6.3 Hz).

*5-Bromo-4-dodecylthiophene-2-carbaldehyde.* To a mixture of N,N-dimethylformamide (27.27 gm, 0.37 mole) and 30 mL of 1,2-dichloroethane at 0°C was added dropwise phosphorus oxychloride (47.26 gm, 0.30 mole). Then the mixture was heated to 35°C and 6.02 gm (0.018 mole) 2-bromo-3-dodecylthiophene was added. After stirring for 24 h at 90°C, the mixture was poured into 300 mL of water and then extracted with chloroform. The organic phase was washed with water repeatedly and dried over $MgSO_4$. The solvent was removed and the residue was purified by column chromatography (EA:Hexane = 5:95) to get an orange liquid (4.82 gm, 74.6 %) $^1$H NMR ($CDCl_3$, 300 MHz): 9.74 (s,

1H), 7.48 (s, 1H), 2.59 (t, 1H, 7.5 Hz), 1.62-1.57 (m, 2H), 1.31-1.25 (m, 18H), 0.87 (t, 3H, 6.6 Hz).

*4'-(5-Bromo-4-dodecylthiophen-2-yl)-2,2':6',2''-terpyridine.* To a solution of 2 acetyl pyridine (3.79 gm, 3.51 mL, 31.3 mmole) in methanol (50 mL), aqueous sodium hydroxide (3.5 gm, 87.5 mmole in 20 mL water) was added dropwise. The reaction mixture was stirred for 30 mins. Then 5-bromo-4-dodecylthiophene-2-carbaldehyde (4.5 gm, 12.52 mmole) in 50 mL of methanol was added drop wise. The reaction mixture was stirred 18 hours at room temperature. The solvent was evaporated off and crude product was extracted from water and dichloromethane. To the above crude an excess of ammonium acetate (35 gm) in 150 mL acetic acid/ethanol (2/1) was added. The reaction mixture was heated to reflux for 30 hours. The mixture was cooled and poured into 500 mL water. Organic phase was extracted by dichloromethane, dried over $MgSO_4$ and the solvent was removed by rotary evaporation. The crude product was purified by neutral alumina column chromatography (DCM : Hexane = 20 : 80) to get pure product as yellow solids (3 gm, 42.5%). $^1$H NMR ($CDCl_3$, 300 MHz): 8.73 (d, 2H, 4.8 Hz), 8.64 (d, 2H, 8.1 Hz), 7.87 (t, 2H, 7.6 Hz), 7.48 (s, 1H), 7.35 (m, 2H), 2.60 (t, 2H, 7.6 Hz), 1.64-1.60 (m, 2H), 1.34-1.25 (m, 18H), 0.86 (t, 3H, 6.9 Hz). $^{13}$C NMR ($CDCl_3$, 300 MHz): 156.53, 156.30, 149.53, 143.99, 143.15, 141.40, 137.29, 127.06, 124.37, 121.73, 116.83, 111.54, 32.32, 30.13, 30.08, 29.97, 29.67, 23.09, 14.53. Elemental analysis for $C_{31}H_{36}BrN_3S$: Calculated : (%) C, 66.18; H, 6.45; N, 7.47; Found: (%)C, 66.57; H, 6.02; N, 7.15. MS (FAB) m/z 561.10 (calcd $(M)^+$: 561.18.

Tris(4-(4,4,5,5-tetramethyl-1,3,2-dioxaborolan-2-yl)phenyl)amine:[8i] $^1$H NMR ($CDCl_3$, 300 MHz): 7.69 (d, 6H, 8.4 Hz), 7.08 (d, 6H, 8.5 Hz), 1.33 (s, 36H).

***TPA3TPY***. In a 100 mL flame-dried two-neck flask fitted with a condenser, tris(4-(4,4,5,5-tetramethyl-1,3,2-dioxaborolan-2-yl)phenyl)amine (0.6 gm, 0.96 mmole), 4'-(5-bromo-4-dodecylthiophen-2-yl)-2,2':6',2''-terpyridine (2 gm, 3.55 mmole) and of tetrakis(triphenylphosphine)palladium (55.65 mg, 0.048 mmole) was added. The mixture was degassed and purged nitrogen. Then, 40 mL of anhydrous toluene and 2M aqueous potassium carbonate solution (8 mL) was added. The reaction mixture was heated to 90°C with vigorous stirring until reaction completion by TLC analyses (~55 hours). The mixture was poured into water (100 mL) and extracted with dichloromethane. The organic layer was washed thrice with water, once with brine and dried over $MgSO_4$. The solvent was evaporated and the residue was purified by neutral alumina column chromatography (DCM : Hexane = 60 : 40) to give pure product as yellow solids (1.17 gm, 75.5%). $^1$H NMR ($CDCl_3$, 300 MHz): 8.76 (d, 6H, 4.7 Hz), 8.68 (s, 6H), 8.67 (d, 6H, 7.9 Hz), 7.88 (t, 6H, 7.6 Hz), 7.69 (s, 3H), 7.48 (d, 6H, 7.4 Hz), 7.38 (t, 6H, 7.8 Hz), 7.29 (s, 6H), 2.76 (t, 6H, 7.14 Hz), 1.73-1.65 (m, 6H), 1.41-1.23 (m, 54H), 0.84 (t, 9H, 6.3 Hz). $^{13}$C NMR ($CDCl_3$, 300 MHz): 156.08, 155.91, 149.07, 146.61, 143.39, 139.78, 139.66, 138.85, 136.81, 133.11, 132.11, 131.98, 131.93, 130.04, 129.05, 128.54, 128.49, 128.38, 124.16, 123.82, 121.29, 116.52, 31.87, 3.06, 29.68, 29.62, 29.51, 29.34, 29.09, 22.65, 14.09. Elemental analysis for $C_{111}H_{120}N_{10}S_3$: Calculated: (%)C, 78.87; H, 7.16; N, 8.29; Found: (%) C, 79.15; H, 7.62; N, 8.53. MS (MALDI-TOF): m/z 1690.08 (calcd $(M)^+$: 1690.40.

*General Procedure for Synthesis of Triple Metal System*

**G-TPY-RuCl3** (3.2 equiv. w.r.t. **TPA3TPY**) and $AgBF_4$ (12.8 equiv. w.r.t. **TPA3TPY**) were taken in acetone (50 mL) and refluxed 36 hours under $N_2$ atmosphere. The solution was filtered to remove AgCl salt. The filtrate was evaporated and to it **TPA3TPY** (1 equiv.) was added. The mixture was dissolved in 5-7 mL dimethyl acetamide and 50 mL n-BuOH and refluxed for 48 hours. The product was cooled and added drop wise into a beaker containing 500 mL MeOH under stirring. The solid was filtered, washed in MeOH and 6:1 mixture of MeOH: acetone. The residue was dried and recrystallized in mixture of acetone:MeOH (1:10) to get desired compounds.

***TPARu3G1.*** Black powder. Yield: 69%. $^1$H NMR (DMSO-$d_6$, 300 MHz): 9.31-9.27 (m, br, 12H), 9.08 (m, br, 12H), 8.77 (s, br, 3H), 8. 66 (s, br, 3H), 8.20-7.86 (m, br, 15H), 7.84 (s, br, 3H), 7.65-7.56 (m, br, 18H), 7.27 (br, 18H), 7.11 (m, br, 6H), 6.88 (m, br, 6H), 2.75-2.70 (m, br, 18H), 1.57-1.47 (m, br, 18H), 1.20 (m, br, 90H), 0.82-0.73 (m, br, 27H). MS (MALDI-TOF): m/z 4186.25 (calcd $(M)^+$: 4184.31).

***TPARu3G2.*** Black Powder. Yield: 61%. $^1$H NMR (DMSO-$d_6$, 300 MHz): 9.34 (m, br, 12H), 9.10-9.07 (m, br, 12H), 8.49 (m, br, 6H), 8.06 (m, br, 12H), 7.89 (m, br, 12H), 7.59-7.48 (m, br, 24H), 7.38-7.28 (m, br, 12H), 7.04-7.02 (m, br, 12H), 6.81-6.78 (m, br, 12H), 2.75-2.73 (m, br, 30H), 1.56-1.44 (m, br, 30H), 1.26-1.21 (m, br, 126H), 0.84-0.78 (m, br, 45H). MS (MALDI-TOF): m/z 5670.24 (calcd $(M)^+$: 5673.73).

***TPARu3G3.*** Black Powder. Yield: 54%. $^1$H NMR ($CDCl_3$, 300 MHz): 8.83 (br, 12H), 8.61 (br, 12H), 8.16 (br, 6H), 7.84 (br, 12H), 7.62-7.26 (br, 24H), 7.25- 7.15 (br, 42H), 6.90 (br, 24H), 6.64 (br, 24H), 2.74 (br, 54H), 1.62 (br, 54H), 1.31-1.25 (br, 246H), 0.87 (br, 33H). MS (MALDI-TOF): m/z 8660.24 (calcd $(M)^+$: 8655.18.

Results and Discussion

Materials and instrumentation

All chemicals and solv**ents** were reagent grades and purchased from Aldrich, ACROS, Fluka, TCI, TEDIA and Lancaster Chemical Co. Toluene, tetrahydrofuran and diethyl ether were distilled over sodium/benzophenone to keep anhydrous before use. Chloroform ($CHCl_3$) was purified by refluxing with calcium hydride and then distilled. If not otherwise specified, the other solvents were degassed by nitrogen 1 h prior to use. Synthesis of 2-(4-hexylthiophen-2-yl)-4,4,5,5-tetramethyl-1,3,2-dioxaborolane and 4,7-dibromo-2,1,3-benzothiadiazole were prepared by following the literature procedures.

$^1$H NMR spectra were recorded on a Bruker DX-300 (300 MHz) spectrometer using $CDCl_3$ and DMSO-$d_6$ solvents. Elemental analyses were performed on a HERAEUS CHN-OS RAPID elemental analyzer. UV-visible absorption spectra were recorded in dilute chloroform solutions ($10^{-6}$ M) on a HP G1103A spectrophotometer. Solid films of UV-vis measurements were spin-coated on quartz substrates from chloroform solutions with a concentration of 10 mg/mL. Cyclic voltammetry (CV) measurements were performed using a BAS 100 electrochemical analyzer with a standard three-electrode electrochemical cell in a 0.1 M tetrabutylammonium hexafluorophosphate ($Bu_4NPF_6$) solution in (acetonitrile) at room temperature with a scanning rate of 100 mV/s. During the CV measurements, the solutions were purged with nitrogen for 30 s. In each case, a carbon working electrode coated with a thin layer of monomers or polymers, a platinum wire as the counter electrode and a silver wire as the quasi-reference electrode were used and Ag/AgCl (3 M KCl) electrode was served as a reference electrode for all potentials quoted herein. The redox couple of ferrocene/ferrocenium ion ($Fc/Fc^+$) was used as an external standard. The corresponding HOMO and LUMO levels were calculated using $E_{ox/onset}$ and $E_{red/onset}$ for experiments in solid films, which were performed by drop-casting films with the similar thicknesses from $CHCl_3$ solutions (ca. 5 mg/mL).

**Synthesis and structural characterization**

Schematic representations and final chemical structures of mono-, bis- and tris-'Ru'-based systems are depicted in Figs. 1-4, respectively. Three generations of thiophene dendrimers (**G1**, **G2** and **G3**) were synthesized.[8f] As shown in Scheme 1, Stille coupling of 4'-(2-bromo-5-thienyl)-2,2',6',2''-terpyridine with **G1**-SnBu3,

**G2**-SnBu3 and **G3**-SnBu3 produced **G1**-TPY, **G2**-TPY and **G3**-TPY, respectively. The single metal system, i.e., **Ru1G1**, **Ru1G2** and **Ru1G3** were prepared according to Scheme 2. The core ligand of the double metal system was prepared by following Scheme 3. The synthetic route for the preparation of the core ligand in the triple metal system was depicted in Scheme 4. All central core ligands and dendritic metal complexes have good solubilities in common organic solvents, such as DCM, THF, EA, DMF and DMA, which led them to have easy processibilities of device fabrications. The chemical structures of metallo-dendritic complexes and their ligands were confirmed by NMR, Maldi-TOF and UV-Vis characterizations. As illustrated in the NMR spectra of Fig. 5, the clear and dramatic downfield shifts of the (3,3")- and (3',5')-terpyridyl signals along with upfield shifts of the (6,6")-terpyridyl signals were observed upon the complexation with Ru metals. In Fig. 6, the peaks at ca. 550 nm of UV-Vis spectra, which depicted a metal to ligand charge transfer (MLCT) peak, further confirmed the complexation of Ru in the metallo-dendritic architecture. Maldi-TOF mass spectra further verified the formation of the desired dendritic metal complexes.

One metal system:

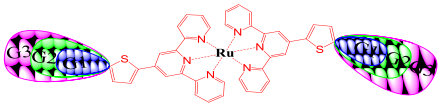


Two metal system:

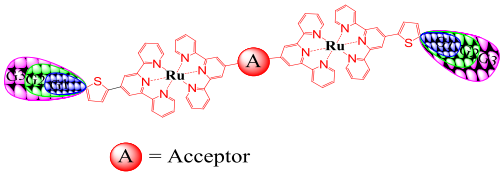


Three metal system:

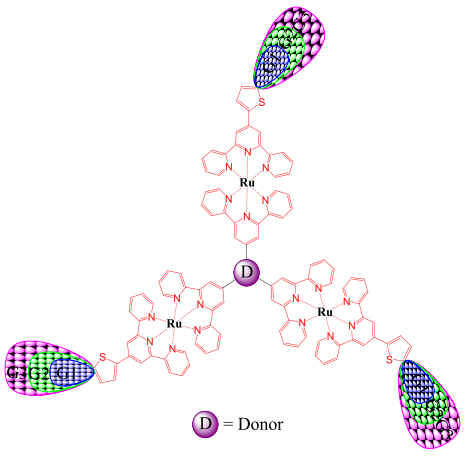


**Fig. 1** Schematic representations of mono-, bis- and tris-'Ru'-based systems.

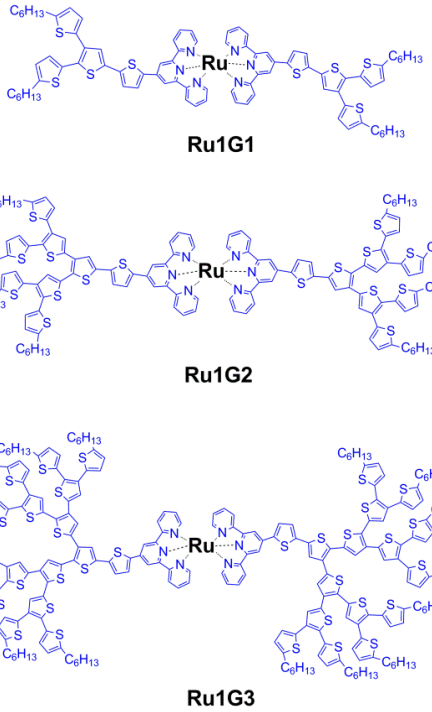


**Fig. 2** Chemical structures of supramolecular mono- (**Ru1G1**, **Ru1G2** and **Ru1G3**).

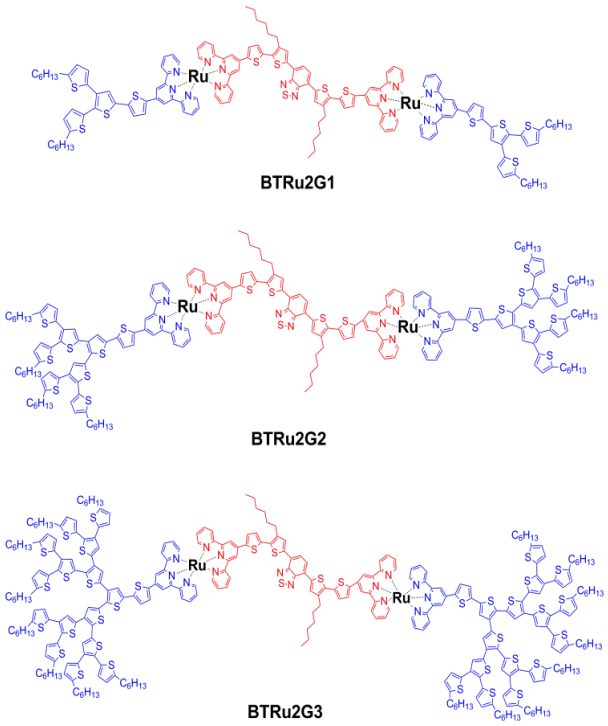


**Fig. 3** Chemical structures of supramolecular bis-(**BTRu2G1**, **BTRu2G2** and **BTRu2G3**).

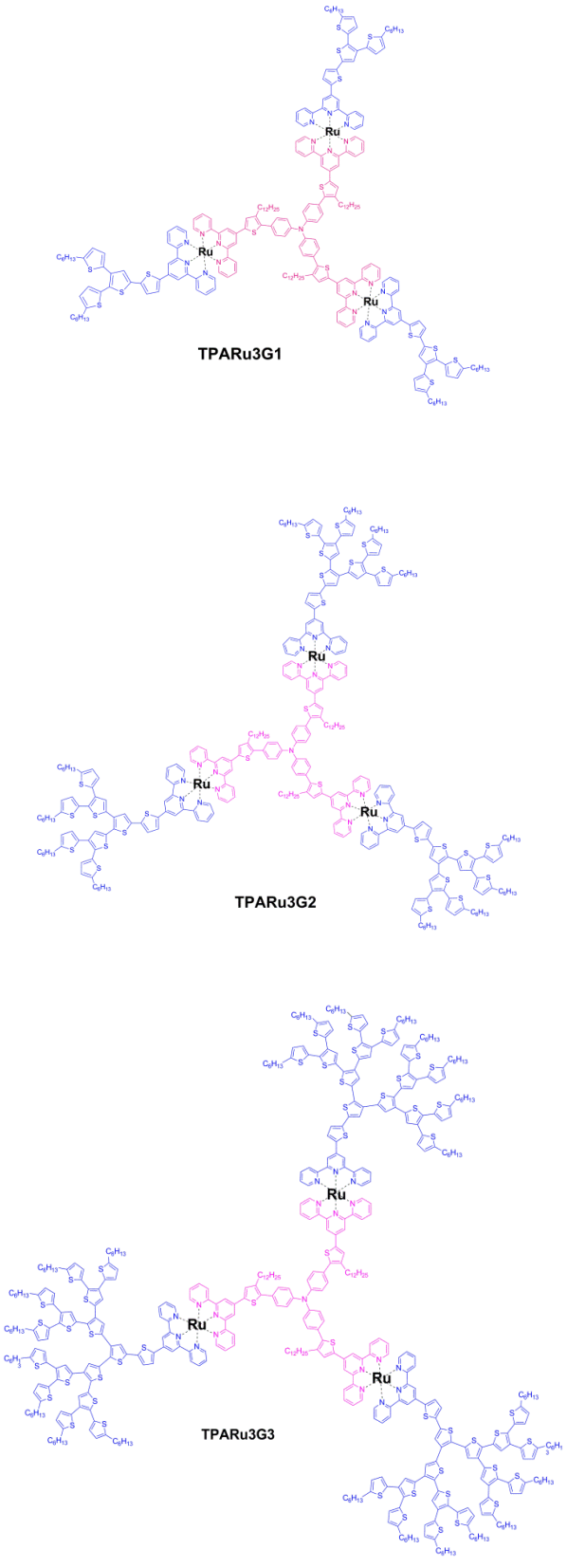


**Fig. 4** Chemical structures of supramolecular tris-'Ru'-based (**TPARu3G1**, **TPARu3G2** and **TPARu3G3**).

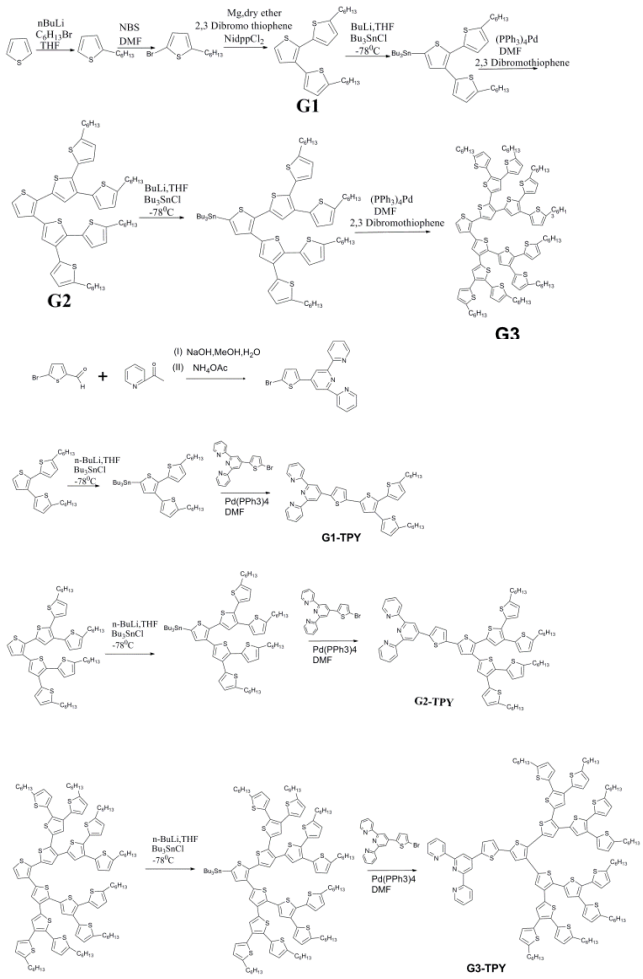


**Scheme 1** Synthetic procedures for different generations of terpyridyl dendritic arms.

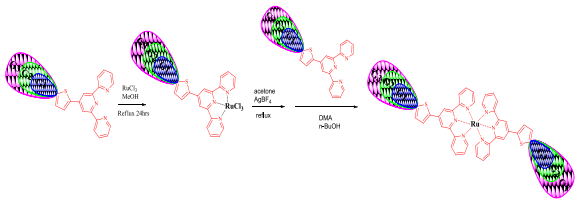

**Scheme 2** Synthesis of the single metal system.

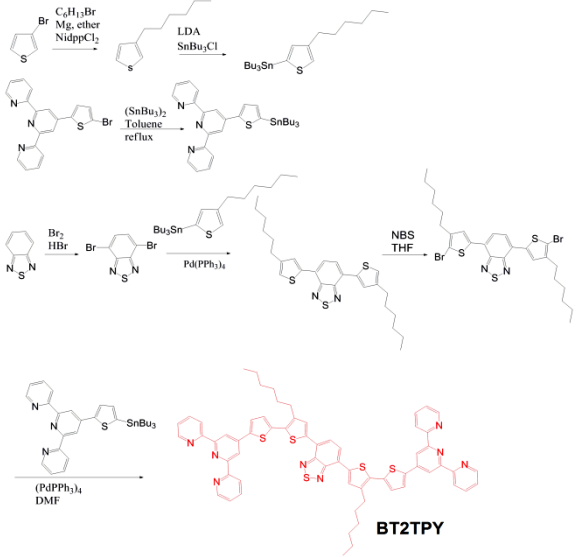


**Scheme 3** Synthesis of the core ligand for the double metal system (**BT2TPY**).

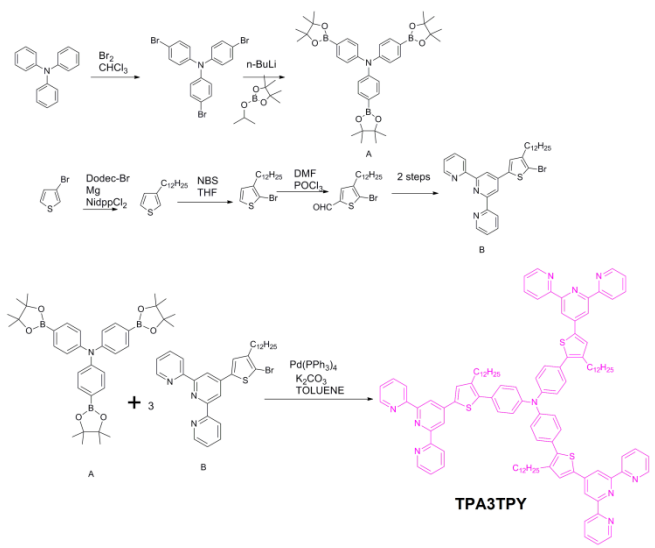


**Scheme 4** Synthesis of the core ligand for the triple metal system (**TPA3TPY**).

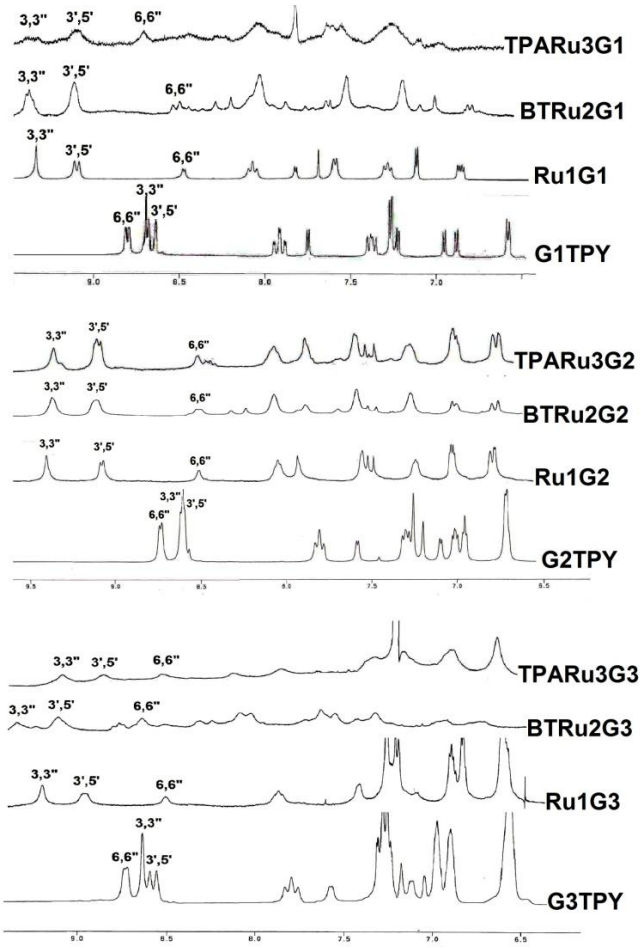


**Fig. 5** NMR spectral characterization for the formation of Ru core.

## Optical and electrochemical properties

The photophysical properties of the mono-, bis- and tris-'Ru'-based dendritic complexes were investigated by UV-Vis absorption spectroscopy in both dilute solutions ($10^{-6}$ M) and spin-coated solid films on quartz substrates. Their absorption wavelengths ($\lambda_{abs}$), optical bandgaps ($E_g^{opt}$) and absorption onsets ($\lambda_{onset}$) in both solutions and film states are summarized in Table 1, where these metallo-dendrimers covered a broad absorption range of 250-750 nm with the optical bandgaps of 1.51-1.86 eV. Fig. 6a shows the absorption spectra of the single metal system (**Ru1G1**, **Ru1G2** and **Ru1G3**) in both solution and film states. The peaks at ~300 nm correspond to π-π* transitions of the terpyridyl moieties. Peaks at ~400 nm evolve from the π-π* transitions in the π-conjugated thiophene dendritic arms. In these Ru(II)-based metallo-dendrimers, self-assembly induced by metal ions was readily observed by the occurrence of an additional absorption band metal-to-ligand charge transfer, i.e., (MLCT) ranging from 500–580 nm, which were resulted from the promotion of an electron from the metal ($Ru^{II}$)-centered d-orbital to unfilled ligand-centered π* orbitals. Peaks at ~550 nm arise from the MLCT of dendritic metal complexes. Fig. 6b shows the absorption spectra of the double metal system (**BTRu2G1**, **BTRu2G2** and **BTRu2G3**) in both solution and film states. In the film state, the MLCT peaks at ~ 550 nm were significantly shifted bathochromically with the concomitant shifts in the absorption onsets. This was attributed to the enhancement of π-π* stacking by the aggregation of neighboring dendritic spramolecular partner in the solid state. Fig. 6c depicts the absorption spectra of the triple metal system (**TPARu3G1**, **TPARu3G2** and **TPARu3G3**) in both solution and film states. Like the double metal system, the MLCT peaks of the tris-'Ru'-based dendritic complexes at ~550 nm were shifted bathochromically with notable shifts in the absorption onsets, which corresponded to the strong intramolecular associations and aggregations in solid films. It is worthy to mention that the absorption of these Ru-based dendritic complexes showed extended absorptions beyond their MLCT peaks. Due to the extended absorptions, these metallo-dendritic complexes possessed small optical bandgaps (1.51-1.86 eV). The optical band gaps showed decreasing trends as increasing the dendrimers' generation (G1-G3)
among all three systems of metallo-dendritic complexes. The double metal system revealed lower optical bandgaps than the other systems (i.e., single and triple metal systems). This can be attributed to the donor-acceptor architecture in the double metal system i.e., **BTRu2G1**, **BTRu2G2**, **BTRu2G3**), which possessing the electron acceptor unit in the benzothiadiazole core ligand caused an efficient intramolecular electron transfer.

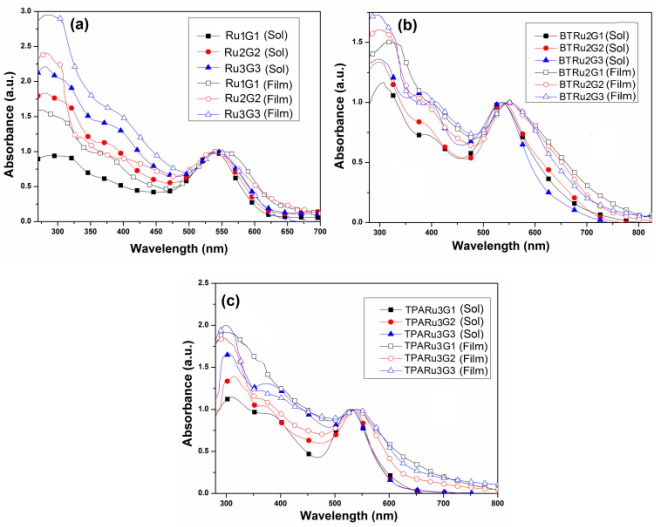


**Fig. 6** UV-Vis absorption spectra of supramolecular dendritic metal complexes in CHCl3 at c = 1 x 10-5 M (solid symbols) and solid films (hollow symbols). (a) mono-, (b) bis- and (c) tris-'Ru'-based systems.

We further investigated the time resolved fluorescence measurements for these three systems of metallo-dendritic complexes probed at 510 nm (excited at 375 nm). The time resolved lifetime spectra of these metallo-dendritic complexes are depicted in Fig. 7. A single exponential fitting for the fluorescence lifetime of the metallo-dendritic complexes, corresponding to the

lifetime of S1 state, are also summarized in Table 1. All these metallo-dendritic complexes showed very diminutive fluorescence lifetime values. However, the fluorescence lifetime values of the single and double metal systems were found to be the largest and smallest, respectively, among these three systems of metallo-dendritic complexes. The lifetime values of double metal system were found to be smallest and the triple metal system showed moderate fluorescence lifetime values. Moreover, it is also observed that the fluorescence lifetime values decreased gradually with higher generations of metallo-dendritic complexes from G1 to G3.

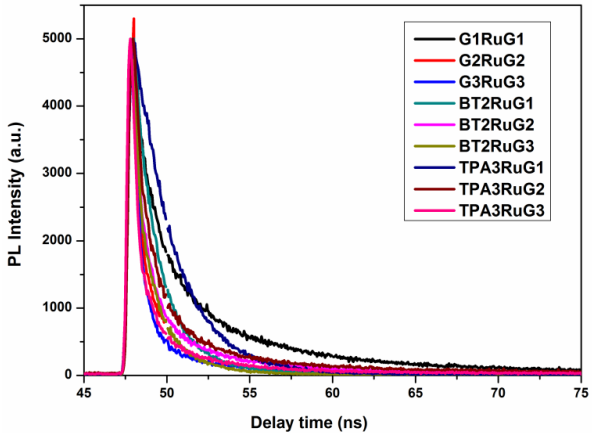


**Fig. 7** Time resolved fluorescence spectra of supramolecular Ru-based dendritic complexes.

**Table 1**. Optical properties of Ru-based dendritic complexes.

| Dendritic complexes | $\lambda_{abs,sol}$ [nm][a] | $\lambda_{abs,film}$ [nm][b] | $\lambda_{onset}$ [nm] | $E_g^{opt}$ [eV][c] | $\tau_{avg}$ [ns][d] |
|---|---|---|---|---|---|
| **Ru1G1** | 537 | 552 | 665 | 1.86 | 6.136 |
| **Ru1G2** | 541 | 543 | 683 | 1.81 | 4.112 |
| **Ru1G3** | 545 | 547 | 691 | 1.79 | 3.021 |
| **BTRu2G1** | 534 | 545 | 786 | 1.57 | 2.351 |
| **BTRu2G2** | 537 | 550 | 797 | 1.55 | 2.039 |
| **BTRu2G3** | 540 | 553 | 816 | 1.51 | 1.604 |
| **TPARu3G1** | 526 | 536 | 711 | 1.74 | 2.972 |
| **TPARu3G2** | 533 | 541 | 750 | 1.65 | 2.505 |
| **TPARu3G3** | 535 | 545 | 772 | 1.60 | 2.003 |

[a] Concentration of $10^{-5}$ M in chloroform solutions. [b] Spin coated from solutions on quartz substrates. [c] Optical band gaps were estimated from the absorption spectra in films by using the equation $E_g = 1240/\lambda_{edge}$. [d] Time resolved fluorescence lifetime.

To survey the electronic properties of these three series of metallo-dendritic complexes, the HOMO and LUMO levels were investigated by CV measurements in solid films with Ag/AgCl as a reference electrode, calibrated by ferrocene ($E_{1/2(ferrocene)}$ = 0.45 mV vs. Ag/AgCl). The CV voltamograms are depicted in Fig. 8 and the energy levels are summarized in Table 2. The HOMO and LUMO levels were estimated by the oxidation and reduction potentials from the reference energy level of ferrocene (4.8 eV below the vacuum level) according to the following equation: $E_{HOMO/LUMO}$ = [-($E_{onset}$ - 0.45) - 4.8] eV. With the increase in the generations of dendritic metal complexes, the electron donating ability of metallo-dendritic complexes increased which resulted in subsequent increases in HOMO levels in each series of metallo-dendritic complexes. The relatively low bandgaps of the double metal system were due to the donor-acceptor architecture of the benzothiadiazole core as an electron acceptor and the thiophene dendritic arms as electron donors. Although there are some deviations in the optical and electrochemical bandgaps, the trend of the bandgaps in the three series of metallo-dendritic complexes is similar.

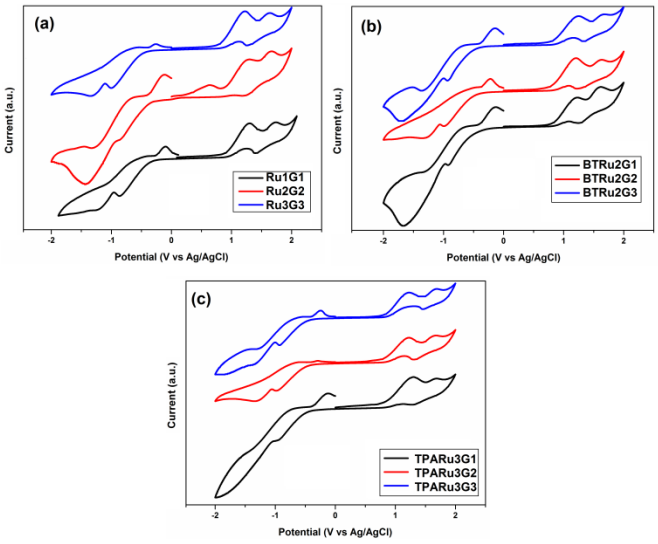


**Fig. 8** CV spectra of Ru-based dendritic complexes in solid films. (a) mono-, (b) bis- and (c) tris-'Ru'-based systems.

**Table 2** Energy levels and bandgaps of Ru-based dendritic complexes.[a]

| Dendritic complexes | $E_{red}$[b] [V] | LUMO[c] [eV] | $E_{ox}$[b] [V] | HOMO[c] [eV] | $E_g^{el}$ [eV] |
|---|---|---|---|---|---|
| **Ru1G1** | -0.59 | -3.75 | 0.92 | -5.27 | 1.52 |
| **Ru1G2** | -0.61 | -3.74 | 0.89 | -5.24 | 1.50 |
| **Ru1G3** | -0.71 | -3.64 | 0.82 | -5.17 | 1.53 |
| **BTRu2G1** | -0.69 | -3.65 | 0.82 | -5.17 | 1.52 |
| **BTRu2G2** | -0.70 | -3.64 | 0.79 | -5.14 | 1.50 |
| **BTRu2G3** | -0.72 | -3.62 | 0.77 | -5.12 | 1.50 |
| **TPARu3G1** | -0.69 | -3.65 | 0.86 | -5.21 | 1.56 |
| **TPARu3G2** | -0.71 | -3.63 | 0.81 | -5.16 | 1.53 |
| **TPARu3G3** | -0.72 | -3.62 | 0.80 | -5.15 | 1.53 |

[a] Reduction and oxidation potentials measured by cyclic voltammetry in solid films. [b] Onset oxidation and reduction potentials. [c] EHOMO /ELUMO= [-(Eonset-0.45)-4.8] eV, where 0.45 V is the value for ferrocene vs. Ag/Ag+ and 4.8 eV is the energy level of ferrocene below the vacuum.

### Device fabrication and photovoltaic properties

To investigate the potential applications of mono-, bis- and tris-Ru(II)-based dendritic complexes in PVCs, the BHJ solar cell devices comprising an active layer of metallo-dendritic complexes as electron donors blended with $PC_{70}BM$ as an electron acceptor were fabricated with a configuration of ITO/PEDOT:PSS(30 nm)/metallo-dendritic complexes:$PC_{70}BM$= 1:1 (w/w) (~80 nm)/Ca(30 nm)/Al(100 nm) and measured under AM 1.5 simulated solar light. The polymer solutions were prepared from metallo-dendritic complexes mixed with $PC_{70}BM$ in chloroform solutions. The current density (J) versus voltage (V) curves of the PVCs are demonstrated in Fig. 9, where the open circuit voltage ($V_{oc}$), short circuit current density (Jsc ), fill factor (FF) and power conversion efficiency (PCE) values are summarized in Table 3. According to the theory, Voc values should depend on the difference between the HOMO levels of the electron donors (i.e., metallo-dendrimers) and the LUMO level of the electron acceptor (i.e., $PC_{70}BM$), but several other parameters would also critically affect the usual trend of $V_{oc}$ values, such as the carrier recombination, the resistance related to the thickness of the active layer and the degree of phase separation between different components in the polymer blend, which could energetically amend the expected $V_{oc}$ values. Therefore, according to the higher generation of the metallo-dendrimers their HOMO levels were

sequentially enhanced, but their corresponding Voc values also increased.[8m-q] This result might be related to the higher efficiency of electron transfer (possessing a shorter life time of PL) induced by the increased electron donor thiophene moieties of the metallo-dendrimers with higher generations. Compared with the single and triple metal systems, the higher efficiencies of the double metal system could be attributed to the presence of dendritic thiophene arms and bis-'Ru'-based core ligand (as electron donor and acceptor moieties, respectively) to induce stronger ICT bands and broader sensitization ranges. This result was originated from the presence of dendritic thiophene arms and bis-'Ru'-based core ligand as electron donor and acceptor moieties, respectively, to induce the stronger ICT and broadening of the sensitization range. According to the above photovoltaic results, the BHJ PSC device containing an active layer of **BTRu2G3**:$PC_{70}BM$=1:1 (w/w) revealed the best PCE value of 0.51, which is consistent with the shortest fluorescence life time of **BTRu2G3** (in Table 1) among all metallo-dendritic complexes. Tris-'Ru'-based architectures with the terthiophene-triphenylamine core ligand showed moderate photovoltaic performance due to their star shaped branched structure possessing deficient electron acceptor moiety in the core ligand.

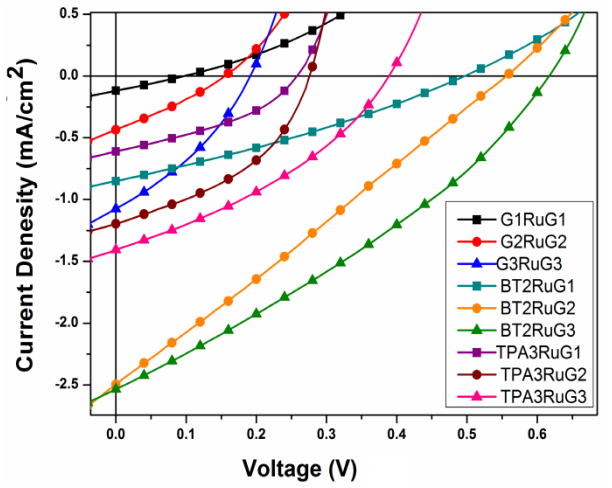


**Fig. 9** Current–voltage curves of BHJ solar cells using blended films of "mono-, bis-, tris-Ru(II)-based metallo-dendritic complexes":$PC_{70}BM$ 1:1 (w/w) under the illumination of AM 1.5G, 100 mW $cm^{-2}$.

**Table 3** Photovoltaic properties of BHJ solar cell devices with a configuration of ITO/PEDOT:PSS/dendritic complex:$PC_{70}BM$=1:1 (w/w)/Ca/Al.[a]

| Active layer[b] Dendritic complex:$PC_{70}BM$ (1:1 w/w) | $V_{oc}$ [V] | $J_{sc}$ [mA/cm$^2$] | FF [%] | PCE [%] |
|---|---|---|---|---|
| **Ru1G1** | 0.10 | 0.12 | 25.0 | 0.003 |
| **Ru1G2** | 0.16 | 0.44 | 28.01 | 0.02 |
| **Ru1G3** | 0.20 | 1.07 | 32.4 | 0.07 |
| **BTRu2G1** | 0.49 | 0.84 | 33.78 | 0.14 |
| **BTRu2G2** | 0.55 | 2.49 | 26.34 | 0.36 |
| **BTRu2G3** | 0.61 | 2.54 | 32.67 | 0.51 |
| **TPARu3G1** | 0.26 | 0.61 | 37.83 | 0.06 |
| **TPARu3G2** | 0.28 | 1.20 | 41.66 | 0.14 |
| **TPARu3G3** | 0.39 | 1.40 | 34.79 | 0.19 |

[a] Measured under AM 1.5 irradiation, 100 mW$cm^{-2}$. [b] Active layer with the weight ratio of Dendritic complex:$PC_{70}BM$ =1:1.

The best two photovoltaic performance of the BHJ PSC cells containing bis-Ru(II)-based dendritic complexes **BTRu2G2** and **BTRu2G3** were further optimized by fabricating the active layer using different weight ratios (i.e., 1:2 and 1:3 w/w) of **BTRu2G2**:$PC_{70}BM$ and **BTRu2G3**:$PC_{70}BM$, which illustrated the J–V curves of the PSC devices in Fig. 10 and their related photovoltaic data are demonstrated in Table 4. The best PCE value of 0.77% with $V_{oc}$= 0.69 V, $J_{sc}$= 3.51 mA/cm$^2$ and FF= 31.89% was obtained in the PSC device containing **BTRu2G3**:$PC_{70}BM$=1:3 (by wt).

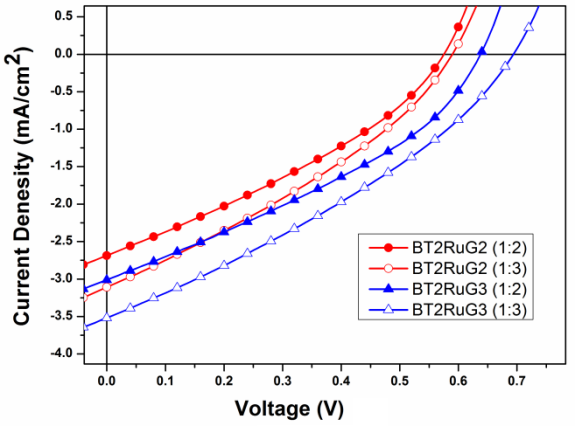


**Fig. 10** Current–voltage curves of BHJ solar cells using an active layer of **BTRu2G2** and **BTRu2G3** blended with $PC_{70}BM$ in two different weight ratios 1:2 & 1:3) under the illumination of AM 1.5G, 100 mW $cm^{-2}$.

**Table 4** Photovoltaic properties of BHJ solar cell devices with a configuration of ITO/PEDOT:PSS/dendritic complex:PC70BM/Ca/Al.[a]

| Active layer Dendritic complex:$PC_{70}BM$ | $V_{oc}$ [V] | $J_{sc}$ [mA/cm$^2$] | FF [%] | PCE [%] |
|---|---|---|---|---|
| **BTRu2G2:$PC_{70}BM$=1:2 (w/w)** | 0.57 | 2.69 | 32.97 | 0.50 |
| **BTRu2G2:$PC_{70}BM$=1:3 (w/w)** | 0.59 | 3.11 | 32.41 | 0.59 |
| **BTRu2G3:$PC_{70}BM$=1:2 (w/w)** | 0.63 | 3.02 | 34.77 | 0.66 |
| **BTRu2G3:$PC_{70}BM$=1:3 (w/w)** | 0.69 | 3.51 | 31.89 | 0.77 |

[a] Measured under AM 1.5 irradiation, 100 mW $cm^{-2}$.

Fig. 11 represents the atomic force microscopic (AFM) images of **BTRu2G2**:$PC_{70}BM$ (1:3) and **BTRu2G3**:$PC_{70}BM$ (1:3), and the root mean square roughnesses ($R_{rms}$) of these images were 8.0 nm and 7.3 nm, respectively. The higher roughness could reduce the charge-transport distance and at the same time providing nano-scaled texture that further enhances internal light scattering and light absorption. However, the Jsc value was decreased in **BTRu2G2**:$PC_{70}BM$ (1:3) compared with **BTRu2G3**:$PC_{70}BM$ (1:3). This is due to the larger $R_{rms}$ of **BTRu2G2**:$PC_{70}BM$ (1:3) than that of **BTRu2G3**:$PC_{70}BM$ (1:3) causing large-scaled phase separation, which decreased the diffusional escape proabilities for mobile charge carriers, and hence to increase the charge recombination, which is consistent with Jsc and PCE values obtained.

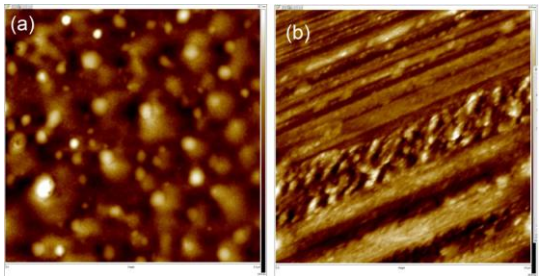


**Fig. 11** AFM images of blended (a) **BTRu2G2**:$PC_{70}BM$ and (b) **BTRu2G3**:$PC_{70}BM$ spin-coated from chloroform in the ratio of 1:3 (w/w).

## Conclusions

Herein, we synthesized three series of mono-, bis- and tris-'Ru'-based supramolecular dendritic metal complexes. Their suitable photophysical and electrochemical properties, such as extended absorption ranges, lower optical as well as electrochemical bandgaps, revealed these metallo-dendritic complexes to be useful for the photovoltaic applications. Tris-'Ru'-based complexes with a terthiophene-triphenylamine core showed moderate photovoltaic performance possibly originated from the non-planar structure of each dendritic branch and thus to cause the hindered electron transport. Compared with the other two series (mono- and tris-'Ru'-based dendritic metal complexes), bis-'Ru'-based dendritic complexes possessed higher PCE values due to the proper molecular design of the donor-acceptor architecture containing a benzothiadiazole-hexyl thiophene core as an electron acceptor moiety. Among the three generations (**G1**-**G3**) of all supramolecular complexes, the larger PCE values were obtained in the higher generation of the metallo-dendritic complexes in each individual mono-, bis- and tris-'Ru'-based series. Therefore, the PSC device containing an active layer of **BTRu2G3**:$PC_{70}BM$=1:3 (by wt), i.e., the third generation of the bis-'Ru'-based dendritic complex **BTRu2G3**, showed the highest PCE value of 0.77%. Compared with our previous report of main-chain Ru(II) metalo-polymers (containing bi-thiophene linkers and benzothiadiazole acceptor) with PCE = 0.45%,[4m] a higher power conversion efficiency (PCE = 0.77%) could be obtained by taking similar benzothiadiazole acceptor and thiophene dendrons in the monodisperse system of **BTRu2G3**. However, the photovoltaic efficiency could be further improved by suitable and selective incorporations of denritic analogues with higher fill factors (improved film qualities) and enhanced short circuit current densities.

## Acknowledgments

The financial support of this project is provided by the National Science Council of Taiwan ROC) through NSC 101-2113-M-009-013-MY2 and NSC102-2221-E-009-174 and National Chiao Tung University through 97W807.

## References

1 (a) H. Choi, M. Kuno, G. V. Hartland and P. V. Kamat, *J. Mater. Chem. A.*, 2013, **1**, 5487; (b) Z. Mu, Q. Shao, J. Ye, Z. Zeng, Y. Zhao, H. H. Hng, F. Y. C. Boey, J. Wu and X. Chen, *Langmuir*, 2011, **27**, 1314; (c) K. E. Erkkila, D. T. Odom and J. K. Barton, *Chem. Rev.*, 1999, **99**, 2777; (d) I. V. Lightcap and P. V. Kamat, *Acc. Chem. Res.*, 2012, DOI:10.1021/ar300248f; (e) F. Barigelletti and L. Flamigni, *Chem. Soc. ReV.*, 2000, **29**, 1; (f) P. Laine´, F. Bedioui, E. Amouyal, V. Albin and F. Burruyer-Penaud, *Chem. Eur. J.*, 2002, **8**, 3162; (g) S. Ott, M. Kritikos, B. Akermark and L. Sun, *Angew. Chem. Int. Ed.*, 2003, **42**, 3285; (h) P. R. Andres and U. S. Schubert, *Ad*V. *Mater.*, 2004, **16**, 1043; (i) N. K. Subbaiyyan, I. Obraztsov, C. A. Wijesinghe, Tran, K, W. Kutner and F. D'Souza, *J. Phys. Chem. C.*, 2009, **113**, 8982; (j) H. Hofmeier, U. S. Schubert, *Chem. Soc. Rev.*, 2004, **33**, 373; (k) G. Bianké and R. Häner, *Chem. Bio. Chem.*, 2004, **5**, 1063; (l) M. Schmittel, V. Kalsani, R. S. K. Kishore, H. Colfen and J. W. Bats, *J. Am. Chem. Soc.*, 2005, **127**, 11544; (m) M. Schmittel, V. Kalsani, P. Mal and J. W. Bats, *Inorg. Chem.*, 2006, **45**, 6370; (n) S. H. Hwang, C. N. Moorefield, L. Dai and G. R. Newkome, *Chem. Mater.*, 2006, **18**, 4019; (o) E. Maligaspe, A. S. D. Sandanayaka, T. Hasobe, O. Ito and F. D'Souza, *J. Am. Chem. Soc.* 2010, **132**, 8158.

2 (a) J.-F. Gohy, B. G. G. Lohmeijer and U. S. Schubert, *Chem. Eur. J.*, 2003, **9**, 3472; (b) E. Puodziukynaite, L. Wang, K. S. Schanze, J. M. Papanikolas and J. R. Reynolds, *Polym. Chem.*, 2014, **5**, 2363; (c) K. Feng, X. Shen, Y. Li, Y. He, D. Huang and Q. Peng, *Polym. Chem.*, 2013,**4**, 5701.

3 (a) A. S. A. E. Aziz, J. L. Pilfold, B. Z. Momeni, A. J. Prouda and J. K. Pearson, *Polym. Chem.*, 2014, DOI: 10.1039/c4py00249k; (b) J.-M. Lehn, *Supramolecular Chemistry, Concept and Perspectives, VCH: Weinheim*, 1995; (c) G. R. Newkome, E. He and C. N. Moorefield, *Chem. Rev.*, 1999, **99**, 1689; (d) U. S. Schubert and C. Eschbaumer, *Angew. Chem. Int. Ed.*, 2002, **41**, 2892; (e) G. R. Newkome, P. Wang, C. Moorefield, T. J. Cho, P. P. Mohapatra, S. Li, S. H. Hwang, O. Lukoyanova, L. Echegoyen, J. A. Palagallo, V. Lancu and S.-W. Hla, *Science*, 2006, **312**, 1782; (f) S. Basak, Y. S. L. V. Narayana, M. Baumgarten, K. Müllen and R. Chandrasekar, *Macromolecules*, 2013, **46**, 362; (g) S. Flores-Torres, G. R. Hutchison, L. J. Soltzberg and H. D. Abruña, *J. Am. Chem. Soc.*, 2006, **128**, 1513; (h) S. Bonnet, J. P. Collin, M. Koizumi, P. Mobian and J. P. Sauvage, *Adv. Mater.*, 2006, **18**, 1239.

4 (a) K. W. Cheng, C. S. C. Mak, W. K. Chan, A. M. C. Ng and A. B. Djurii, *J. Polym. Sci. Part A: Polym. Chem.*, 2008, **46**, 1305; (b) K. K. Y. Man, H. L. Wong, W. K. Chan, C. Y. Kwong and A. B. Djurisic, *Chem. Mater.*, 2004, **16**, 365; (c) P. D. Vellis, J. A. Mikroyannidis, C. N. Lo and C. S. Hsu, *J. Polym. Sci. Part A: Polym. Chem.*, 2008, **46**, 7702; (d) V. Duprez, M. Biancardo, H. Spanggaard and F. C. Krebs, *Macromolecules*, 2005, **38**, 10436; (e) O. Hagemann, M. Jørgensen and F. C. Krebs, *J. Org. Chem.*, 2006, **71**, 5546; (f) K. K. Y. Man, H. L. Wong, W. K. Chan, A. B. Djurisic, E. Beach and S. Rozeveld, *Langmuir*, 2006, **22**, 3368; (g) Y. Pan, B. Tong, J. Shi, W. Zhao, J. Shen, J. Zhi and Y. Dong, *J. Phys. Chem. C.*, 2010, **114**, 8040; (h) V. Stepanenko, M. Stocker, P. Muller, M. Buchner and F. Wurthner, *J. Mater. Chem.*, 2009, **19**, 6816; (i) Y. Y. Chen, Y. T. Tao and H. C. Lin, *Macromolecules*, 2006, **39**, 8559; (j) W. S. Huang, Y. H. Wu, H. C. Lin and J. T. Lin, *Polym. Chem.*, **2010**, **1**, 494; (k) J. F. Yin, D. Bhattacharya, Y. C. Hsu, C. C. Tsai, K. L. Lu, H. C. Lin, J. G. Chen and K. C. Ho, *J. Mater. Chem.*, 2009, **19**, 7036; (l) J. F. Yin, J. G. Chen, Z. Z. Lu, K. C. Ho, H. C. Lin and K. L. Lu, *Chem. Mater.*, 2010, **22**, 4392; (m) H. Padhy, D. Sahu, I. H. Chiang, D. Patra, D. Kekuda, C. W. Chu and H. C. Lin, *J. Mater. Chem.*, 2011, **21**, 1196; (n) J. F. Yin, J. G. Chen, J. T. Lin, D. Bhattacharya, Y. C. Hsu, H. C. Lin, K. C. Ho and K. L. Lu, *J. Mater. Chem.*, 2012, **22**, 130.

5 (a) P. D. Vellis, J. A. Mikroyannidis, C. N. Lo, C. S. Hsu, *J. Polym. Sci. Part A: Polym. Chem.*, 2008, **46**, 7702; (b) H. Padhy, D. Sahu, I. H. Chiang, D. Patra, D. Kekuda, C. W. Chu and H. C. Lin, *J. Mater. Chem.*, 2011, **21**, 1196; (c) H. Padhy, M. Ramesh, D. Patra, R. Satapathy, M. K. Pola, H. C. Chu, C. W. Chu, K. H. Wei and H. C. Lin, *Macromolecular Rapid Comm.*, 2012, **33**, 528; (d) N. K. Subbaiyan, C. A. Wijesinghe and F. D'Souza, *J. Am. Chem. Soc.*, 2009, **131**, 14646; (e) S. Deng, G. Krueger, P. Taranekar, S. Sriwichai, R. Zong, R. Thummel, R. Advincula, *Chem. Mater.*, 2011, **23**, 3302; (f) S. Caramori, J. Husson, M. Beley, C. A. Bignozzi, R. Argazzi and P. C. Gros, *Chem. Eur. J.*, 2010, **16**, 2611.

6 (a) R. J. Kline, M. D. McGehee, E. N. Kadnikova, J. S. Liu and J. M. J. Fre´chet, *Adv. Mater.*, 2003, **15**, 1519; (b) P. Schilinsky, U. Asawapirom, U. Scherf, M. Biele and C. J. Brabec, *Chem. Mater.*, 2005, **17**, 2175; (c) X. N. Yang, J. Loos, S. C. Veenstra, W. J. H. Verhees, M. M. Wienk, J. M. Kroon, M. A. J. Michels and R. A. J. Janssen, *Nano Lett.*, 2005, **5**, 579; (d) N. Kopidakis, W. J. Mitchell, J. Van-de-Lagemaat, D. S. Ginley, G. Rumbles, S. E. Shaheen and W. L. Rance, *Appl. Phys. Lett.*, 2006, **89**, 103524; (e) A. M. Nardes, A. J. Ferguson, J. B. Whitaker, B. W. Larson, R. E. Larsen, K. Maturova, P. A. Graf, O. V. Boltalina, S. H. Strauss and N. Kopidakis, *Adv. Funct. Mater.*, 2012, **22**, 5900; (f) E. Maligaspe, A. S. D. Sandanayaka, T. Hasobe, O. Ito and F. D'Souza, *J. Am. Chem. Soc.*, 2010, **132**, 8158; (g) M. I. Mangione and R. A. Spanevello, *Macromolecules*, 2013, **46**, 4754; (h) K. Chiad, M. Grill, M. Baumgarten, M. Klapper and M. Müllen, *Macromolecules*, 2013, **46**, 3554; (i) G. Vamvounis, P. E. Shaw and P. L. Burn. *J. Mater. Chem. C.*, 2013, **1**, 1322; (j) S. A. Ponomarenko, N. N. Rasulova, Y. N. Luponosov, N. M. Surin, M. I. Buzin, I. Leshchiner, S. M. Peregudova and A. M. Muzafarov, *Macromolecules*, 2012, **45**, 2014; (k) O. V. Rud, A. A. Polotsky, T. Gillich, O.V. Borisov, F. A. M. Leermakers, M. Textor and T. M. Birshtein, *Macromolecules*, 2013, **46**, 4651; (l) C. Q. Ma, E. M. Osteritz, M. Wunderlin, G. Schulz and P. Bauerle, *Chem. Eur. J.*, 2012, **18**, 12880; (m) K. Mutkins, S. S. Y. Chen, A. Pivrikas, M. Aljada, P. L. Burn, P. Meredith and B. J. Powell, *Polym. Chem.*, 2013, **4**, 916; (n) J. You, G. Li and Z. Wang, *Polymer*, 2012, **53**, 5116; (o) H. Ye, D. Chen, M. Liu, X. Zhou, S. J. Su and Y. Cao, *Polymer*, 2013, **54**, 162.

7 (a) T. Hasobe, Y. Kashiwagi, M. A. Absalom, J. Sly, K. Hosomizu, M. J. Crossley, H. Imahori, P. V. Kamat and S. Fukuzumi, *Adv. Mater.*, 2004, **16**, 975; (b) R. Bettignies, Y. Nicolas, P. Blanchard, E. Levillain, J. M. Nunzi and J. Roncali, *Adv. Mater.*, 2003, **15**, 1939; (c) N. Satoh, T. Nakashima and K. Yamamoto, *J. Am. Chem. Soc.*, 2005, **127**, 13030; (d) T. Kengthanomma, P. Thamyongkit, J. Gasiorowski, A. M. Ramil and N. S. Sariciftci, *J. Mater. Chem.*, 2013, DOI: 10.1039/c3ta11095h. (e) M. J. Cho, J. Seo, K. Luo, K. H. Kim, D. H. Choi and P. N. Prasad, *Polymer*, 2012, **53**, *3835.*

8 (a) G. R. Newkome and C. N. Moorefield, F. Vögtle, *Dendrimers and dendrons: concepts, syntheses, applications. Weinheim: Wiley-VCH*, 2001; (b) J. M. J. Fréchet and D. A. Tomalia, *Dendrimers and other dendritic polymers. Chi-chester: Wiley*, 2002; (c) M. Kawa and J. M. J. Fréchet, *Chem. Mater.*, 1998, **10**, 286; (d) C. J. Hawker and J. M. J. Fréchet, *J. Am. Chem. Soc.*, 1992, **114**, 8405; (e) V. Maraval, R. Laurent, B. Donnadieu, M. Mauzac, A. M. Caminade and J. P. Majoral, *J. Am. Chem. Soc.*, 2000, **122**, 2499; (f) C. Xia, X. Fan, J. Locklin and R. C. Advincula, *Org. Lett.*, 2002, ***4***, 2067; (g) W. J. Mitchell, A. J. Ferguson, M. E. Köse, B. L. Rupert, D. S. Ginley, G. Rumbles, S. E. Shaheen and

N. Kopidakis, *Chem. Mater*. 2009, **21**, 287; (h) A. C. Kanarr, B. L. Rupert, S. Hammond, J. van-de-Lagemaat, J. C. Johnson and A. Ferguson, *J. Phys. Chem., A*., 2011, **115**, 2515; (i) J. Cremer and P. Bauerle, *J. Mater. Chem*., 2006, **16**, 874 ; (j) S. Deng, T. M. Fulghum, G. Krueger, D. Patton, J. Y. Park and R. C. Advincula, *Chem. Eur. J*., 2011, **17**, 8929; (k) A. Mishra, A. M. Osteritz and P. Bäuerle, *Beilstein J. Org. Chem*., 2013, **9**, 86; (l) G. L. Schulz, M. Mastalerz, C. Q. Ma, M. Wienk, R. Janssen and P. Bäuerle, *Macromolecules*, 2013, **46**, 2141; (m) Y. Li, H. Li, B. Xu, Z. Li, F. Chen, D. Feng, J. Zhang and W. Tian, *Polymer*, 2010, **5**, 1786; (n) H. Chung, T. Narita, J. Yang, P. Kim, M. Takase, M. Iyoda and D. Kim, *Chem. Eur. J*., 2013, **19**, 9699; (o) V. Tamilavan, M. Song, R. Agneeswari, J.-W. Kang, D.-H. Hwang and M. H. Hyun, *Polymer*, 2013, **54**, 6125; (p) E. Kozma, D. Kotowski, F. Bertini, S. Luzzati and M. Catellani, *Polymer*, 2010, **51**, 2264; (q) Y. Sun, B. Lin, H. Yang and X. Gong, *Polymer*, 2012**, 53**, 1535; (r) D. Sahu, C. H. Tsai, H. Y. Wei, K. C. Ho, F. C. Chang and C. W. Chu, *J. Mater. Chem.*, 2012, **22**, 7945; (s) J. M. Jiang, H. C. Chen, H. K. Lin, C. M. Yu, S. C. Lan, *Polym. Chem*., 2013, **4**, 5321; (t) *S. C. Lan, P. A. Yang, M. J. Zhu, C. M. Yu, J. M. Jiang, K. H. Wei, Polym. Chem*., 2013, **4**, 113; (u) V. Tamilavan, M. Song, S.-H. Jin and M. H. Hyun, *Polymer*, 2011, **52**, 2384.

TOC

The polymer solar cell device containing an active layer of **BTRu2G3**:$PC_{70}BM$=1:3 (by wt), i.e., the third generation of the bis-'Ru'-based dendritic complex **BTRu2G3**, showed the highest PCE value of 0.77%.

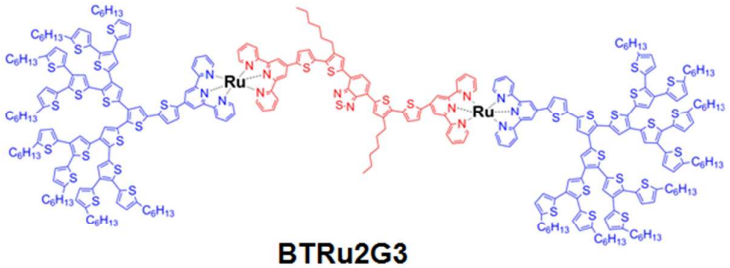


**BTRu2G3**

**$\eta$ = 0.77%**